

The atomic Bose gas in Flatland

Z. Hadzibabic , P. Krüger , M. Cheneau , B. Battelier and J. Dalibard

Laboratoire Kastler Brossel, Ecole normale supérieure, 24 rue Lhomond, 75005 Paris, France

Abstract. We describe a recent experiment performed with rubidium atoms (^{87}Rb), aiming at studying the coherence properties of a two-dimensional gas of bosonic particles at low temperature. We have observed in particular a Berezinskii–Kosterlitz–Thouless (BKT) type crossover in the system, using a matter wave heterodyning technique. At low temperatures, the gas is quasi-coherent on the length scale set by the system size. As the temperature is increased, the loss of long-range coherence coincides with the onset of the proliferation of free vortices, in agreement with the microscopic BKT theory.

1. INTRODUCTION

The type of phase transitions that a physical system can undergo depends crucially on its dimensionality. In a three-dimensional (3D) system, one usually observes the emergence of a long range order below a critical temperature. The corresponding order parameter can be constant in space, like the macroscopic wave function of a 3D Bose-Einstein condensate (BEC) or the magnetization in a 3D ferromagnetic material. In a two-dimensional fluid, long-range order is destroyed by thermal fluctuations at any finite temperature T . In particular, for a 2D uniform ideal gas of identical bosons it is well known that BEC cannot occur at a non-zero temperature.

However in an interacting 2D Bose gas, there exists a certain critical temperature T_c at which a phase transition takes place. Below T_c correlations of the order parameter decay only algebraically in space and the system is superfluid. Above T_c the correlations decay exponentially and superfluidity is lost. The Berezinskii-Kosterlitz-Thouless (BKT) paradigm [1, 2] associates this transition with the emergence of a topological order embodied in the pairing of vortices with opposite circulations. For $T < T_c$ vortices are only found as part of bound pairs, whereas for $T > T_c$ unbound vortices proliferate and cause the exponential decay of the correlations of the order parameter.

This behavior is characteristic of a variety of 2D phenomena including the superfluidity in liquid helium films [3], the superconducting transition in arrays of Josephson junctions [4], and the collision physics of 2D atomic hydrogen [5]. Here we report experimental evidence for BKT-type phenomenon in harmonically trapped dilute atomic gases. Specifically, we analyze series of interference patterns between independent quasi 2D gases of ^{87}Rb atoms. We identify a temperature region close to the predicted T_c , around which the phase coherence of the gas evolves rapidly with T . For temperatures above this transition region, phase defects indeed proliferate. Our observations thus pave the way to a direct, quantitative confirmation of the microscopic basis of the BKT theory.

The paper is organized as follows. We first present (section 2) our experimental

configuration in order to set the scale of parameters of our quasi-2D gas. We then review the relevant known results for homogeneous (section 3) and trapped (section 4) Bose gases in two dimensions. In section 5 we present our main experimental results concerning the observation of a BKT type crossover in a 2D gas of rubidium atoms.

2. EXPERIMENTAL SYSTEM

Our experimental setup has been described in detail in [6, 7] (see [8] for other recent experiments performed with quasi-2D atomic gases). We start our experiment with a magnetically trapped, quantum degenerate 3D cloud of ^{87}Rb atoms. A 1D optical lattice with a period of $d = 3\text{ }\mu\text{m}$ along the vertical direction z is used to split the 3D gas into two independent clouds and to compress them into the 2D regime.

The two clouds form parallel, elongated 2D strips, characterized by the harmonic trapping frequencies in the xy plane $\omega_x = (2\pi) = 11\text{ Hz}$ and $\omega_y = (2\pi) = 130\text{ Hz}$. The oscillation frequency in the lattice potential along the z direction is $\omega_z = (2\pi) = 36\text{ kHz}$, and the tunneling between the two planes is negligible on the time-scale of the experiment.

The maximal number of atoms in each planar quasi-condensate is $5 \cdot 10^4$. The Thomas-Fermi approximation presented in section 4 yields $\rho_c = 10^{10}\text{ cm}^{-2}$ for the central density of each quasi-condensate, and $2R_x = 120\text{ }\mu\text{m}$ and $2R_y = 10\text{ }\mu\text{m}$ for the x and y lengths of the strips, respectively. The corresponding chemical potential is $\mu = \hbar = 18\text{ kHz}$. Since $\mu < \hbar\omega_z$, the motion along z is frozen out.

In quasi-2D, the chemical potential can be written as

$$\mu = \frac{\hbar^2}{M} \tilde{g} \rho_c ; \quad (1)$$

where M is the atomic mass, and the dimensionless parameter \tilde{g} can be expressed in terms of the 3D scattering length $a = 5.2\text{ nm}$ and the extension of the ground state along the lattice direction $a_z = \frac{\hbar}{M\omega_z} = 0.17\text{ }\mu\text{m}$

$$\tilde{g} = \frac{8\pi}{a} \frac{a}{a_z} \approx 0.15 ; \quad (2)$$

Since $\tilde{g} < 1$, each planar cloud is a weakly interacting system. The healing length $\xi = \frac{\hbar}{\sqrt{2M\mu}} = \frac{1}{\sqrt{2\tilde{g}\rho_c}} \approx 0.2\text{ }\mu\text{m}$ gives the characteristic size of the core of a vortex, and the quantity $\pi = 2\tilde{g} \approx 0.3$ can be interpreted as the number of atoms in the area $\pi\xi^2$ that are missing in the vortex core. Note that strictly speaking \tilde{g} also depends on the relevant energy set by the chemical potential μ [9, 10, 11], but for our experimental parameters this dependence may be neglected.

3. THE HOMOGENEOUS 2D GAS

In this section we give a brief summary of the known results concerning a 2D gas of bosonic particles. Consider first an ideal gas of N bosons at temperature T , confined in

a square box of size L^2 . Using the Bose-Einstein distribution and assuming a smooth variation of the population of the various energy states, we find a relation between the spatial density $\rho = N/L^2$, the thermal wavelength $\lambda = h/(2\pi M k_B T)^{1/2}$ and the chemical potential μ :

$$\rho \lambda^2 = \frac{1}{e^{\mu/(k_B T)}} \quad ;$$

This relation allows one to derive the value of μ for any value of the degeneracy parameter $\rho \lambda^2$. It indicates that no condensation takes place in 2D, contrary to the 3D case. In the latter case the relation between $\rho^{(3D)} \lambda^3$ and μ ceases to admit a solution above a critical value of $\rho^{(3D)} \lambda^3$, which is the signature for BEC. The absence of BEC in two dimensions remains valid for an interacting gas with repulsive interactions [12, 13].

In spite of the absence of BEC, the physics of an interacting, homogeneous 2D gas is still very rich. One can show that at sufficiently low temperature the gas has a superfluid component of density ρ_s [1, 2, 14]. When temperature increases, both the thermal wavelength λ and the superfluid fraction decrease until the product $\rho_s \lambda^2$ reaches the critical value

$$T = T_c \quad ; \quad \rho_s \lambda^2 = 4 \quad ; \quad (3)$$

The superfluid density then suddenly drops to zero, and the gas becomes normal [14]. The phase transition also manifests itself in the 1-body correlation function for the atomic field $g_1(r) = \langle \psi^\dagger(r) \psi(0) \rangle$. Below T_c one expects a power law decay:

$$T < T_c \quad ; \quad g_1(r) \propto r^{-1/(2\rho_s \lambda^2)} \quad ; \quad (4)$$

reaching $g_1(r) \propto r^{-1/4}$ for $T = T_c$, whereas $g_1(r)$ decays exponentially for $T > T_c$.

We now discuss the physical phenomenon at the origin of this phase transition [1, 2]. We use a simple modeling of the system, which consists in neglecting density fluctuations of the gas to deal only with phase fluctuations. At low temperature the phase varies smoothly with position and can be expanded in normal modes. This amounts to consider only phonon excitations of the system. Using the equipartition theorem, one can derive the algebraic decay of the g_1 function given in (4). When the temperature increases, other excitations like quantized vortices start to play a significant role. A quantized vortex is a point where the density is zero and around which the phase rotates by a multiple of 2π . For our purpose it is sufficient to consider only singly charged vortices, where the phase varies by 2π around the vortex core. The Berezinskii-Kosterlitz-Thouless phase transition, occurring at $T = T_c$ (see (3)), corresponds to the following mechanism:

- For $T < T_c$ the free vortices are absent. Vortices exist in the system only in the form of bound pairs, formed by two vortices with opposite circulations. The contribution of these vortex pairs to the decay of the correlation function g_1 is negligible, and the algebraic decay of g_1 is dominated by the phonons.
- For $T > T_c$, the free vortices form a disordered gas of phase defects, which are responsible for the exponential decay of g_1 .

Neglecting density fluctuations allows for a qualitative understanding of the BKT transition, but does not provide the relation between the total density ρ and the superfluid

density ρ_s . This question has been addressed in [15] in the limit of an ultra weakly interacting gas ($\ln(\ln(1/\tilde{g})) \rightarrow 1$). The case of weak, but more realistic interactions, has been addressed numerically in [16] and gives $\rho_s/\rho = 4/\ln(\zeta/\tilde{g}) \approx 0.5$ for our parameters (the dimensionless number ζ is found numerically ≈ 380).

4. THE TRAPPED GAS

Consider now a gas of N particles confined by the potential $V(\mathbf{r}) = M(\omega_x^2 x^2 + \omega_y^2 y^2)/2$ in the xy plane. The presence of a trap modifies the density of states and BEC is predicted to occur for an ideal gas when the temperature is below the critical temperature T_0 [17]:

$$N = \frac{\pi^2}{6} \frac{k_B T_0}{\hbar \bar{\omega}} \bar{\omega}^2 = \omega_x \omega_y : \quad (5)$$

However it should be pointed out that condensation is a very fragile phenomenon in a 2D harmonic potential. To illustrate this we calculate the spatial density $\rho(\mathbf{r})$ using the semiclassical approximation. Starting with the expression for the phase space density

$$w(\mathbf{r}; \mathbf{p}) = \frac{1}{h^2} \frac{1}{\exp((\frac{p^2}{2m} + V(\mathbf{r}) - \mu)/k_B T) + 1} ;$$

we obtain

$$\rho(\mathbf{r}) = \int w(\mathbf{r}; \mathbf{p}) d^2 p = \frac{1}{\lambda^2} \ln(1 + e^{(\mu - V(\mathbf{r}))/k_B T}) ;$$

Taking $\mu \rightarrow 0$ to reach the condensation threshold, we find

$$\rho_{\max}(\mathbf{r}) \lambda^2 = \ln(1 + e^{V(\mathbf{r})/k_B T_0}) ;$$

Integrating $\rho_{\max}(\mathbf{r})$ over the whole space, we recover the threshold (5). However, we also note that $\rho_{\max}(0) = \infty$. This suggests that condensation in a 2D harmonic potential requires an infinite 2D spatial density at the trap center, a criterion which cannot be fulfilled as soon as repulsive interactions play a significant role. Note that this is in sharp contrast with the case of a 3D harmonically trapped Bose gas, where condensation occurs when $\rho_{\max}^{(3D)}(0) \approx 2.612/\lambda^3$, which is finite and (within the semi-classical approximation) equal to the threshold density in a homogenous system. We refer the reader to [18, 19] for a detailed discussion of this subject and a collection of recent references.

In the limit of large atom numbers and low temperature, we can still determine the equilibrium shape of the gas by looking at the balance between the trapping potential and the repulsive interatomic potential (Thomas-Fermi approximation). We assume that the atomic gas forms a quasi-condensate [20, 21, 16, 22], so that $\hbar(\hat{\psi}^\dagger(\mathbf{r}))^2(\hat{\psi}(\mathbf{r}))^2 \approx \hbar\hat{\psi}^\dagger(\mathbf{r})\hat{\psi}(\mathbf{r}) \approx \rho_c^2(\mathbf{r})$. We then get an atomic distribution varying as an inverted parabola

$$\rho_c(\mathbf{r}) = \rho_c(0) \left(1 - \frac{x^2}{R_x^2} - \frac{y^2}{R_y^2}\right) ; \quad \frac{\hbar^2}{M} \tilde{g} \rho_c(0) = \mu ;$$

where the chemical potential μ and the radii of the clouds R_i , $i = x, y$ are:

$$\mu = \hbar \bar{\omega} (N \tilde{g} = \pi)^{1/2} \quad \omega_i R_i = \sqrt{\frac{\mu}{2M}} :$$

In the regime where $N \tilde{g} \gg 1$, the chemical potential is much larger than $\hbar \bar{\omega}$ and the dynamics of the gas at low energy is dominated by phonons. One then recovers several features of the homogeneous 2D gas [23]. In particular for $\xi \gg r \gg R_x, R_y$, the correlation function $g_1(r) = \langle \psi^\dagger(r) \psi(0) \rangle$ decays algebraically at low temperature with exponent $1 = (\rho_c(0) \lambda^2)$ (see eq. (2.59) in [23]). A crossover to a true BEC occurs when the decay of g_1 over the sizes R_x, R_y of the quasi-condensate is negligible.

Harmonically trapped gaseous samples are finite in size and have non-uniform density. For these reasons, one does not expect to observe a sharp BKT transition to superfluidity, but rather a smoothed out crossover. However, an interesting question is whether, at least in principle, in the thermodynamic limit one could observe a signature of a sharp transition in a harmonic trap. For simplicity we consider an isotropic trapping ($\omega_x = \omega_y = \bar{\omega}$) and define the thermodynamic limit by taking $N \rightarrow \infty$ and $\omega \rightarrow 0$, while keeping $N\omega^2$ constant. We can then duplicate the Kosterlitz-Thouless argument [2] to find the probability for having a free vortex appearing close to the center of the quasi-condensate under the influence of thermal fluctuations. We choose as a sample region the central disk of radius εR , with $\varepsilon \ll 1$ and kept constant as $R \rightarrow \infty$. The kinetic energy of the gas due to a free vortex in the center of the trap is related to the superfluid density $\rho_s(r)$, which we assume to be close to the quasi-condensate density $\rho_c(r)$ [24]

$$E_K = \frac{1}{2} \int \frac{\hbar^2}{Mr} \rho_s(r) d^2r = \frac{\pi \hbar^2}{M^2} \rho_s(0) \ln(R=\xi) :$$

The entropy associated with the possible choices for the location of a free vortex of size ξ in the disk of radius εR is $S = k_B \ln((\varepsilon R)^2 = \xi^2) = 2k_B [\ln(R=\xi) + \ln(\varepsilon)]$. Therefore in the limit $R=\xi \gg 1=\varepsilon \ll 1$, the free energy $F = E_K - TS$ associated with a free vortex in the central disk of radius εR varies as

$$\frac{F}{k_B T} = \frac{1}{2} \rho_s(0) \lambda^2 - 4 \ln(R=\xi) : \quad (6)$$

We thus expect a rapid variation of the average number of vortices present in the central region when $\rho_s(0) \lambda^2$ varies around 4. When $F > 0$ (i.e. $\rho_s(0) \lambda^2 > 4$) the probability to get a free vortex in this region is small, as the energy cost for a free vortex dominates over the gain in entropy. On the contrary for $F < 0$, i.e. $\rho_s(0) \lambda^2 < 4$, we expect a proliferation of free vortices around the center of the trap and a jump of the local superfluid density to zero, in analogy with the homogenous system. Finally, note that even for $\rho_s(0) \lambda^2 > 4$, free vortices can appear in the periphery of the condensate, because the energy cost for an off-centered vortex is lower. The role of these outer vortices on the coherence properties at the center of the condensate remains to be studied.

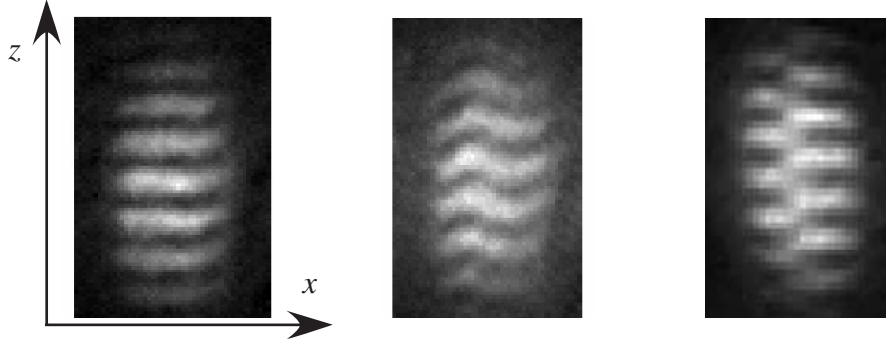


FIGURE 1. Examples of interference patterns between two quasi 2D Bose gases. Left: low temperature pattern; Middle: high temperature pattern; Right: example of a dislocated pattern revealing the presence of a vortex in one of the two planes.

5. EXPERIMENTAL STUDY

5.1. Matter wave heterodyning

In order to study the phase coherence of our quasi-2D gases, we have implemented a matter-wave heterodyning technique. When all confining potentials are suddenly turned off the two clouds expand predominantly perpendicular to the xy plane. As they overlap, a 3D matter wave interference pattern forms with a spatial period $D = 2\pi\hbar t = \langle nd \rangle$ along the z direction, where t is the time-of-flight (TOF) duration [25]. After $t = 20$ ms, the projection of the 3D interference pattern onto the xz plane is recorded on a camera, using a resonant probe laser directed along y .

Three examples of interference patterns are shown in fig. 1. The left pattern is typical of what is obtained at very low temperature, with nearly straight fringes. The middle pattern has been obtained for a larger temperature and the presence of phase fluctuations in the two planes is revealed by the waviness of the interference fringes. Finally we occasionally observe patterns with one (or several) dislocation(s), such as the one shown in the right of fig. 1. We interpret such a dislocation as the signature of a free vortex in one of the two atomic clouds [26, 27]. The matter wave heterodyning technique thus offers a way to study both long wavelength excitations (phonons) by analyzing the smooth variations of the fringes of the interference patterns, and the point-like defects such as free vortices by looking for sharp dislocations in the fringes.

5.2. Extracting g_1 from interference patterns

We use in this paragraph a simple modeling, where we assume that the two gases have the same uniform amplitude ψ_0 and independently fluctuating phases $\varphi_a(x;y)$ and $\varphi_b(x;y)$. The interference signal recorded after TOF is

$$S(x;z) \propto 2\psi_0^2 + e^{2i\pi z=D} c(x) + e^{-2i\pi z=D} c^*(x) \quad (7)$$

with

$$c(x) = \frac{\psi_0^2}{L_y} \int_{L_y=2}^Z e^{i(\varphi_a(x,y) - \varphi_b(x,y))} dy : \quad (8)$$

At this stage the integration distance L_y is arbitrary, and it can differ from the total length $2R_y$ along the y direction. For a quantitative analysis of long-range correlations as a function of temperature, we adopt the method proposed in [28]. The idea is to integrate the coefficient $c(x)$ appearing in (7) over a variable length L_x :

$$C(L_x) = \frac{1}{L_x} \int_{L_x=2}^Z c(x) dx$$

and average $\langle C(L_x) \rangle$ over many images recorded in the same conditions. Using the fact that the phases φ_a and φ_b are uncorrelated, we obtain:

$$\begin{aligned} \langle C(L_x) \rangle^2 &= \frac{1}{L_x^2} \int_{L_x=2}^Z \langle c(x) c(x^0) \rangle dx dx^0 \\ &= \frac{\psi_0^2}{L_x^2 L_y^2} \int_{L_x=2}^Z \int_{L_x=2}^Z \langle e^{i(\varphi_a(x,y) - \varphi_a(x^0,y^0))} e^{i(\varphi_b(x,y) - \varphi_b(x^0,y^0))} \rangle dx dx^0 dy dy^0 \\ &= \frac{1}{L_x} \int_{L_x=2}^Z \langle g_1(x;0) \rangle^2 dx \propto \frac{1}{L_x^{2\alpha}} ; \end{aligned} \quad (9)$$

where we have assumed $L_x = L_y$. The long-range physics is then captured in a single parameter, the exponent α . It is straightforward to understand the expected values of α in some simple cases. In a system with true long-range order, g_1 would be constant and the interference fringes would be perfectly straight. In this case $\alpha = 0$, corresponding to no decay of the contrast upon integration. In the low temperature regime, where g_1 decays algebraically (see (4)) the exponent α coincides with that of g_1 . In the high temperature case, where g_1 decays exponentially on a length scale much shorter than L_x , the integral in (9) is independent of L_x . In this case $\alpha = 0.5$, corresponding to adding up local interference fringes with random phases. The BKT mechanism corresponds to a transition between a power law with exponent $(1 - (\rho_s \lambda^2))^{-1} \approx 0.25$ to an exponential decay of g_1 . It should thus manifest itself in a uniform system as a sudden jump of α from 0.25 to 0.5 when the temperature varies around T_c .

5.3. Experimental results

In order to apply the method of [28] to our data, we fit the density distribution recorded after TOF with a function

$$F(x;z) = G(x;z) [1 + c(x) \cos(2\pi z - D + \theta(x))] ;$$

where $G(x;z)$ is a gaussian envelope, and we proceed with the experimental $c(x)$ as discussed above. We average $\langle C(L_x) \rangle^2$ over 100 images and fit it with the function $L_x^{-2\alpha}$. We have plotted in fig. 2a the results for α , as a function of the average central

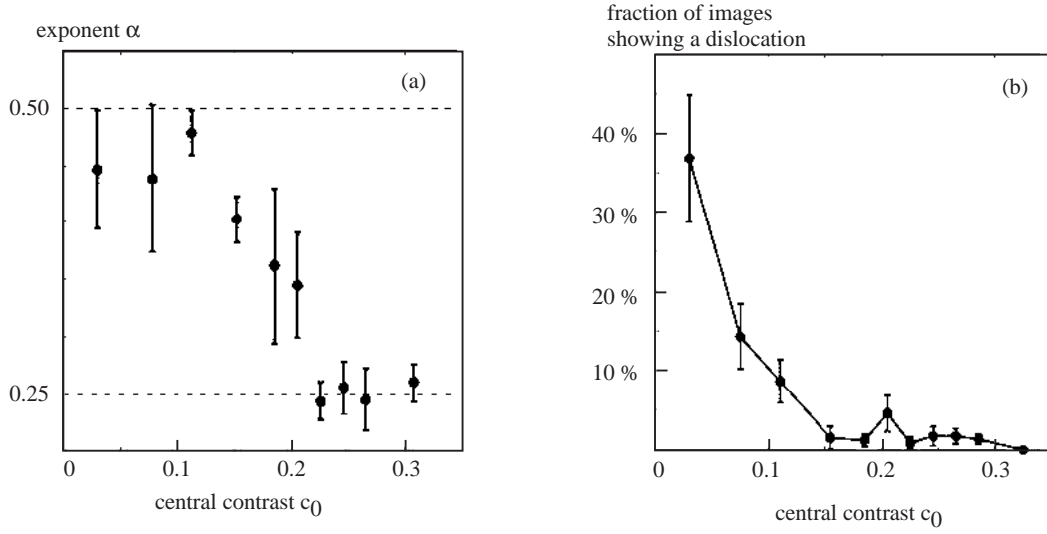


FIGURE 2. (a) Fitting exponent α as a function of the average central contrast c_0 . (b) Fraction of images showing at least one dislocation as a function of c_0 .

contrast c_0 of the images. We choose the latter quantity as a temperature label since we feel that it is less model-dependent than other estimates, based for example on the tails of the atomic TOF distribution. Starting at high temperatures, for values of c_0 ranging from a few % (experimental limit of detectability) up to about 13%, α is approximately constant and close to 0.5. When the temperature is reduced further, α rapidly drops to about 0.25, and for even lower temperatures (larger c_0) it levels off. We thus clearly observe a transition between two qualitatively different regimes at high and low temperatures. The values of α above and below the transition are in agreement with the theoretically expected jump at the BKT transition in a uniform system.

Figure 2b shows the number of sharp dislocations at different temperatures. For the count we consider only the central, $30 \mu\text{m}$ wide region of each image, which is smaller than the length of our smallest quasi-condensates. We observe a clear onset of dislocation proliferation with increasing temperature, and this onset coincides with the loss of quasi-long range coherence described by the rapid variation of α .

We can also independently estimate the cloud's temperature and quasi-condensate density at the onset of quasi-long-range coherence. For images with $c_0 = 0.15$, we get $\rho_c \lambda^2 = 6 \pm 2$ [7]. This is in agreement with the BKT theory, and we refer the reader to [16] for a further discussion on the difference between ρ_c and ρ_s .

5.4. Discussion and summary

The experimental procedure presented here constitutes a powerful technique to study the properties of quasi-2D atomic gases at ultra-low temperature. Our results show that, in agreement with the prediction of the BKT theory, there exists a relatively narrow temperature domain over which the coherence of our trapped planar Bose gas varies

rapidly, with the exponent α in (9) switching from ≈ 0.25 (low temperature side) to ≈ 0.5 (high temperature side). In addition the matter wave heterodyning technique allows for the direct observation of dislocations of the interference pattern due to vortices, and it supports the notion that the unbinding of vortex-antivortex pairs is the microscopic mechanism destroying the quasi-long range coherence in 2D systems.

However, we should point out that the quantitative agreement between our results and the predictions of [28] derived from BKT theory might be partly fortuitous. Indeed though we concentrated on the quasi-uniform part of the images, the geometry effects in our elongated samples ($R_x \approx 12R_y$) could still be important. In particular the integration length L_y in our experiment is equal to the full width of the system $2R_y$ in that direction. The condition $L_x \approx L_y$ used to derive (9) then implies that we probe the planar system on a distance scale L_x that is large compared to its other dimension $2R_y$. Over this length scale the system acquires some quasi-one dimensional features and g_1 is expected to decay exponentially, possibly with a very large coherence length (see e.g. [29]). If this is indeed the case, our experiment is detecting a rapid change of the decay length of the exponential, rather than a change in the functional form of g_1 given in (4). The elongated nature of our samples also changes the quantitative calculation of the threshold for the apparition of a vortex (see section 4). Finally we note that we detect here only a subset of vortices, i.e. those which are well isolated and close to the center of the cloud. The heterodyning technique is not well adapted to the detection of large numbers of vortices, that are expected for temperatures notably above T_c . In the latter case indeed, the fringe pattern becomes hardly detectable and thermally activated phonon modes with a very short wavelength along x can also have a significant contribution. Our work should then be considered as a first step in the investigation of the BKT mechanism in planar atomic gases. A quantitative theoretical analysis of our system will probably require a numerical study, for example along the lines of [30]. In parallel, future experimental studies could be performed with more isotropic samples, and could use a “slicing method” similar to [25] in order to extract local information from the center of the cloud.

ACKNOWLEDGMENTS

We thank E. Altman, E. Demler, M. Lukin, A. Polkovnikov, P.-S. Rath, D. Stamper-Kurn, and S. Stock for useful discussions. We acknowledge financial support by IFRAF, ACI nanoscience, ANR, the Alexander von Humboldt foundation (P.K.) and the EU under Marie-Curie Fellowships (Z.H. and P.K.). Laboratoire Kastler Brossel is a research unit of Ecole normale supérieure and Université Paris 6, associated to CNRS.

REFERENCES

1. V. L. Berezinskii, *Sov. Phys. JETP* **34**, 610-616 (1972).
2. J. M. Kosterlitz and D. J. Thouless, *J. Phys. C* **6**, 1181-1203 (1973).
3. D. J. Bishop and J. D. Reppy, *Phys. Rev. Letters* **40**, 1727-1730 (1978).
4. D. J. Resnick, J. C. Garland, J. T. Boyd, S. Shoemaker, and R. S. Newrock, *Phys. Rev. Letters* **47**, 1542-1545 (1981).

5. A. I. Safonov, S. A. Vasilyev, I. S. Yasnikov, I. I. Lukashevich, and S. Jaakkola *Phys. Rev. Letters* **81**, 4545-4548 (1998).
6. S. Stock, Z. Hadzibabic, B. Battelier, M. Cheneau, and J. Dalibard, *Phys. Rev. Letters* **95**, 190403 (2005).
7. Z. Hadzibabic, P. Krüger, M. Cheneau, B. Battelier, and J. Dalibard, *Nature* **441**, 1118 (2006).
8. A. Görlitz et al., *Phys. Rev. Letters* **87**, 130402 (2001); V. Schweikhard, I. Coddington, P. Engels, V. P. Mogendorff, and E. A. Cornell, *Phys. Rev. Letters* **92**, 040404 (2004); D. Rychtarik, B. Engeser, H. C. Nägerl, and R. Grimm, *Phys. Rev. Letters* **92**, 173003 (2004); N. L. Smith, W. H. Heathcote, G. Hechenblaikner, E. Nugent, and C. J. Foot, *J. Phys. B* **38**, 223-235 (2005); C. Orzel, A. K. Tuchman, M. L. Fenselau, M. Yasuda, and M. A. Kasevich, *Science* **291**, 2386-2389 (2001); S. Burger et al, *Europhys. Letters* **57**, 1-6 (2002).
9. S. K. Adhikari, *Am. J. Phys.* **54**, 362-367 (1986).
10. D. S. Petrov, M. Holzmann, and G. V. Shlyapnikov, *Phys. Rev. Letters* **84**, 2551-2554 (2000).
11. D. S. Petrov and G. V. Shlyapnikov, *Phys. Rev. A* **64**, 012706 (2001).
12. N. D. Mermin and H. Wagner, *Phys. Rev. Letters* **17**, 1133-1136 (1966).
13. P. C. Hohenberg, *Phys. Rev.* **158**, 383-386 (1967).
14. D. R. Nelson and J. M. Kosterlitz, *Phys. Rev. Letters* **39**, 1201-1205 (1977).
15. D. S. Fisher and P. C. Hohenberg, *Phys. Rev. B* **37**, 4936-4943 (1988).
16. N. Prokof'ev, O. Ruebenacker, and B. Svistunov, *Phys. Rev. Letters* **87**, 270402 (2001).
17. V. Bagnato and D. Kleppner, *Phys. Rev. A* **44**, 7439-7441 (1991).
18. J. P. Fernandez and W. J. Mullin, *J. Low Temp. Phys.* **128**, 233-249 (2002).
19. M. Holzmann, G. Baym, J.-P. Blaizot, and F. Laloë, cond-mat/0508131.
20. V. N. Popov, *Functional Integrals in Quantum Field Theory and Statistical Physics*, Reidel, Dordrecht (1983).
21. Yu. Kagan, B. V. Svistunov, and G. V. Shlyapnikov, *Sov. Phys. JETP* **66**, 314 (1987).
22. J. O. Andersen, U. Al Khawaja, and H. T. C. Stoof, *Phys. Rev. Letters* **88**, 070407 (2002).
23. D. S. Petrov, D. M. Gangardt, and G. V. Shlyapnikov, *J. Physique IV France* **116**, 5-44 (2004).
24. The distinction between superfluid density ρ_s and quasi-condensate density ρ_c is delicate. We refer the reader to [16], where the difference between the two quantities is discussed.
25. M. R. Andrews et al., *Science* **275**, 637-641 (1997).
26. S. Inouye et al., *Phys. Rev. Letters* **87**, 080402 (2001).
27. F. Chevy, K. Madison, V. Bretin, and J. Dalibard, *Phys. Rev. A* **64**, 031601(R) (2001).
28. A. Polkovnikov, E. Altman, and E. Demler, *Proc. Natl. Acad. Sci. USA* **103**, 6125-6129 (2006).
29. F. Gerbier, *Europhys. Letters* **66**, 771 (2004).
30. T. P. Simula and P. B. Blakie, *Phys. Rev. Letters* **96**, 020404 (2006).